

An inter-order comparison of copepod fatty acid composition and biosynthesis in response to a long-chain PUFA-deficient diet along a temperature gradient

Robyn Sahota (✉ robyn.sahota@ugent.be)

Ghent University: Universiteit Gent <https://orcid.org/0000-0002-1498-7200>

Jens Boyen

Ghent University: Universiteit Gent

Ilias Semmouri

Ghent University: Universiteit Gent

Samuel Bodé

Ghent University: Universiteit Gent

Marleen De Troch

Ghent University: Universiteit Gent

Research Article

Keywords: Copepods, fatty acids, bioconversion, compound-specific stable isotope analysis, climate change

Posted Date: May 16th, 2022

DOI: <https://doi.org/10.21203/rs.3.rs-1530735/v1>

License:   This work is licensed under a Creative Commons Attribution 4.0 International License.

[Read Full License](#)

Abstract

Copepods serve as a major link in marine food webs, bridging the energy transfer from primary producers to higher trophic levels. Oceanic warming is linked to reduced concentrations of essential fatty acids (FA) in phytoplankton, and it remains unknown if copepods have the capacity to endure. The calanoid *Temora longicornis*, dominant in the Belgian part of the North Sea, and the harpacticoid *Platychelipus littoralis*, abundant in the Paulina mudflat, Westerscheldt, Netherlands, were chosen to analyze the FA biosynthesis response to a polyunsaturated FA (PUFA) deficient diet (*Dunaliella tertiolecta*) along a temperature gradient. Copepods were fed *D. tertiolecta* labelled with the stable isotope carbon-13 (^{13}C) to quantify carbon assimilation and *de novo* FA production at 11, 14, 17, 20, and 23°C. *P. littoralis* did not assimilate *D. tertiolecta* carbon readily, and consequently did not exhibit high bioconversion rates. *T. longicornis* displayed higher rates of *de novo* biosynthesis of eicosapentaenoic acid (EPA, 20:5 ω 3) and docosahexaenoic acid (DHA, 22:6 ω 3) than *P. littoralis* at all temperatures, apart from DHA at 23°C. The calanoid copepod had reduced survival with warming, whereas the harpacticoid copepod exhibited higher and steady survival across the thermal gradient. Although the rate of bioconversion was not adequate to recover the absolute ω 3-content to field concentrations for both species, the relative EPA content (fraction of total FA) in *P. littoralis* did not change between the field and the incubated samples. This suggests that *P. littoralis* was able to maintain the required fraction of EPA necessary for survival at higher temperatures, whereas *T. longicornis* could not. This study highlights *P. littoralis*' short-term resilience, and quantifies the different bioconversion capabilities of both copepods exposed to environmental stressors.

1. Introduction

Record temperature increases and large fluctuations are undisputedly becoming more ordinary and frequent in marine ecosystems (Stenseth et al. 2002)– pressuring the adaptive and acclimatization limits of organisms who have limited motility. These temperature changes can restructure the base of complex marine food webs notably through range-shifts (Beaugrand et al. 2002; McGinty et al. 2021), changes in reproductive timing (Daase et al. 2013), abundances and size (Garzke et al. 2015), and via the modification of individuals' fatty acid (FA) composition (Garzke et al. 2016). This adjustment of primary producer food quality, specifically the predicted reduction of omega(ω)-3 FAs with warming, can have major implications on the availability of these important essential FAs (EFAs) (Hixson and Arts 2016; Colombo et al. 2020). EFAs (e.g. eicosapentaenoic acid (EPA): 20:5 ω 3, docosahexaenoic acid (DHA): 22:6 ω 3) are critical for growth and survival and cannot be produced *de novo* by marine invertebrates in the considerable amounts required (Bell et al. 2007). However, many metazoans possess these biosynthesis capabilities, which were previously disregarded, but now have been resolved with detailed molecular and isotope tracing methods (Kabeya et al. 2018). Cyclopoid, calanoid, and harpacticoid copepod species were shown to possess these biosynthesis capabilities (De Troch et al. 2012; Nielsen et al. 2020), intensified under warming pressures (Werbrouck et al. 2017; Helenius et al. 2020a). Long-chain polyunsaturated FA (LC-PUFA) are defined by a FA chain length of 20 or more carbon units (Ratnayake

and Galli 2009). LC-PUFA biosynthesis is enabled by a series of fatty acyl desaturases (FADS), which introduce a double bond in the FA carbon chain, and the enzymes responsible for elongation, including the catalyzing elongases, which elongate very long chain FA (ELOVL) by introducing two additional carbon atoms in the chain at a time (Bell and Tocher 2009; Monroig and Kabeya 2018). While front-end desaturases and elongases are present throughout copepod orders (Nielsen et al. 2019; Lee et al. 2020; Kabeya et al. 2021), methyl-end desaturases – enabling bioconversion of monounsaturated FAs (MUFAs) towards LC-PUFAs – have recently been detected in at least harpacticoid, cyclopoid and siphonostomatoid copepods, completely revising the current assumptions on global *de novo* LC-PUFA production within aquatic food webs (Kabeya et al. 2018). This ability for bioconversion has been proposed to be a potential adaptive mechanism to overcome reduced dietary LC-PUFA availability (Nielsen et al. 2020), however the triggers/circumstances for bioconversion and the extent to which individuals can offset these deficiencies remains unknown.

Copepods are a dominant group of zooplankton and play an important role due to their high lipid concentrations in comparison to primary producers (Kattner and Hagen 2009), providing higher trophic levels with an energetic food source. In marine intertidal sediments the order Harpacticoida dominates, due to high inputs of detritus and nutrients stimulating microphytobenthos growth, and availability of benthic microbial communities (Meyer 1994; Cnudde et al. 2015). Harpacticoids are a lipid-rich dietary item for demersal and juvenile fish species (Gee 1987; Coull 1990), and can enrich sediment with organic matter, promoting biogeochemical cycling processes (Stock et al. 2014). Comparatively, in the pelagic environment the order Calanoida is the major group within the zooplankton community, serving as prey-items for (larval) fish (Beaugrand et al. 2003; Turner 2004), seabirds (Frederiksen et al. 2013; Bertram et al. 2017), and even whales (Cronin et al. 2017). Apart from direct consumption, they also contribute to the detrital food web through the microbial remineralization (Lampitt et al. 1990), and to the biological carbon pump (Jónasdóttir et al. 2015). Although morphologically distinct, these two orders fill a similarly critical niche in energy transfer, within their respective oceanic realms, and will face analogous warming pressures.

Global sea surface temperatures (SSTs) are expected to rise between 1.2 to 3.47°C by 2100 as per Shared Socioeconomic Pathway (SSP) scenarios 2.6 and 8.5, respectively (Kwiatkowski et al. 2020). Since zooplankton have a relatively short generational time and are poikilothermic, the population dynamics and energetics tied to environmental warming are meaningful (Richardson 2008). This environmental pressure can have an effect on both the organism itself and the algae they consume. Hence, assessing the effects of dietary LC-PUFA provision along a temperature gradient in these important primary consumers is relevant to understand future climate effects on the marine food web. Both temperature and food quality have been shown to be the stressors with the largest impact on individual FA composition (Deschutter et al. 2019), thereby impacting energy flow changes for higher trophic levels. A methodology being used to quantify the transfer of FA incorporation and bioconversion in a consumer is compound-specific stable isotope analysis (CSIA). By labelling the food source with the stable isotope carbon-13 (^{13}C), we are able to track the percent of algae-derived FA under experimental conditions, and,

thereby, we understand differential incorporation or modification/bioconversion processes for each FA (Twining et al. 2020). These data are resolved via gas chromatography combustion isotope ratio mass spectrometry (GC-c-IRMS), allowing us to ascertain the $^{13}\text{C}/^{12}\text{C}$ ratio of individual FAs found within the copepod consumer. Accordingly, the amount of FA in the consumer, derived from the isotopically labelled food source can be determined. As LC-PUFAs are absent in the chlorophyte *Dunaliella tertiolecta*, this alga was selected. As such, the LC-PUFA with *D. tertiolecta* derived carbon in the copepod consumer can be used to assess LC-PUFA biosynthesis during the lab incubation (*de novo*). This method is a proposed alternative FA tracer method to liposomes (Bell et al. 2007).

The objective of this study was to measure the effects of a LC-PUFA deficient diet on the FA composition, incorporation and *de novo* bioconversion in two copepod species of different orders along a temperature gradient. Using 7-day lab treatments, we evaluated the temperature-specific response of carbon incorporation in consumer FAs under LC-PUFA-deficient conditions between *Platychelipus littoralis*, a benthic harpacticoid species with known temperature-dependent bioconversion capabilities (Werbrouck et al. 2017), and the calanoid *Temora longicornis*, the dominant zooplankton species in the southern North Sea (Semmour et al. 2021), with as of yet unknown bioconversion capabilities. While calanoids were often believed to have poor bioconversion capacities (Moreno et al. 1979; Bell et al. 2007), more recent research suggest that at least some species have the ability to produce LC-PUFAs from precursors in ecologically relevant quantities (Nielsen et al. 2019). This study fills the gap of the knowledge of the FA response and bioconversion capabilities in calanoid and harpacticoid orders of copepods under the same experimental temperature conditions.

2. Materials And Methods

2.1. Sampling and experimental design

Adults of the calanoid copepod *T. longicornis* (Müller, 1785) were collected from the Belgian part of the North Sea (BPNS), on the research vessel (RV) Simon Stevin on 15th February 2021 at sampling station 330 (51°25' 995" N, 2°48'41.5" E) in the coastal waters near Ostend. Copepods were collected using a vertically towed WP2 net (57 cm diameter, 200 µm mesh size), towed from bottom to surface (SST: 4.8°C, 32.997 PSU, 0 µg L⁻¹ chlorophyll a). Individuals were transported and held in 35 L vessels, containing natural seawater obtained from the sampling station. Adults of the harpacticoid copepod *P. littoralis* (Brady, 1880) were obtained during low tide from the Paulina intertidal mudflat, Westerscheldt estuary, Netherlands (51°21' 24" N, 3° 42' 51"E) on 9 March 2021. The top sediment layer was sampled (5.45°C, 21.55 PSU), and individuals were isolated by sieving through a 250 µm mesh. Adult copepods were randomly selected under a Wild Heerbrugg M5 stereomicroscope. To characterize the FA profile and carbon content of individuals in the field, quadruplicates of 50 and 20 copepods, respectively, were sampled and stored at -80°C after allowing gut clearance for 12 h in autoclaved filtered natural seawater (FNSW). Following identification to species level, adult individuals (n = 60: *T. longicornis*, n = 70: *P. littoralis*) were placed directly in 1 L glass jars of autoclaved FNSW with aeration for 12 h at 11°C to allow

gut clearance before addition of the food. No aeration was added to the *P. littoralis* experimental jars, as without sediment the benthic copepods would be disturbed beyond natural conditions.

The chlorophyte, *Dunaliella tertiolecta* (Butcher, 1959), was obtained from the Laboratory of Aquaculture & Artemia Reference Center at Ghent University, and cultured at 15°C in autoclaved FNSW with NutriBloom Plus. *D. tertiolecta* was isotopically labelled with 16.8 mg NaH¹³CO₃ stock solution per 100 mL of growth medium (De Troch et al. 2012; Werbrouck et al. 2017). The stock cultures were grown in climate rooms (15°C, 12:12h light:dark, 17–46 photons m⁻² s⁻¹) for 10 days prior to the experiment. Average culture cell concentrations were determined with a Beckman Coulter counter Multisizer 3. In the calanoid experiment, 25 mL of algae were transferred to 50 mL falcon tubes for each replicate, to achieve approximately 25 000 cells mL⁻¹ inside the experimental unit (0.248 ± 0.078 mg carbon L⁻¹), ensuring non-limiting food concentrations (Koski and Klein Breteler 2003; Arendt et al. 2005; Veloza et al. 2006). The falcon tubes were centrifuged (10 min, 10°C, RCF = 3500 g), the supernatant containing the ¹³C label and nutrients was removed, and *D. tertiolecta* was resuspended in autoclaved FNSW. This was repeated twice, after which the falcon tubes were stored without light for 12 h at 4°C prior to the treatment to inhibit further algal growth (De Troch et al. 2012; Werbrouck et al. 2017). In the harpacticoid experiment, *D. tertiolecta* culture flasks were prepared similarly as above, however then combined to reach non-limiting food concentrations; 11 mL were added to each experimental unit, thereby containing approximately 25 000 cells mL⁻¹ (1.098 ± 0.089 mg carbon L⁻¹). Quadruplicate 10 mL samples of *D. tertiolecta* were taken from separate culture flasks for FA analysis, centrifuged (10 min, 10°C, RCF = 3220 g), and supernatant removed. The resulting concentrated 1 mL sample was transferred to a glass 10 mL vial and stored at -80°C. Additional samples were taken for total carbon analysis by filtering 25 mL onto GF/F paper and stored at -80°C. Algae concentrations were measured approximately 12 h after addition to the experimental units and after 6 days.

Thermal gradient experiments were conducted on *T. longicornis* and *P. littoralis*. Quadruplicates of 60 and 70 adults of *T. longicornis* and *P. littoralis*, respectively, were placed in glass jars filled with 1 L of autoclaved FNSW and fed *ad libitum* (10 000–25 000 cells mL⁻¹) with the prepared ¹³C-labelled *D. tertiolecta*. Experimental units were exposed to five different temperature treatments (11, 14, 17, 20, 23°C) in temperature controlled Lovibond TC-175 incubators (± 1°C) for 6 days under a 12:12 h light:dark regime. These treatments were acclimated from 11°C to their treatment temperature at a rate of 2°C h⁻¹. To assess potential algae growth throughout the experiments, quadruplicate 1 L jars of autoclaved FNSW containing only *D. tertiolecta* were placed in the 14°C incubator for the duration of the experiment. No increase in cell concentration was reported in these samples (Figure S1), hereafter we assume algae growth was successfully inhibited. On day 6 of the experiment, individuals were sieved on a 38 µm mesh and living individuals were counted and transferred to fresh autoclaved FNSW to allow gut clearance for 24 h. After this period, surviving individuals were transferred to glass vials and stored at -80°C prior to FA analysis. If more than 40 or 50 individuals survived during the calanoid and harpacticoid experiment respectively, additional samples were taken for carbon isotope analysis. These individuals were stored at -80°C prior to stable isotope sample preparation.

2.2. Bulk ^{13}C stable isotope analysis

Individuals were washed three times in MilliQ, removing particles attached to the cuticula, then placed in Elemental Microanalysis Pressed Tin Capsules (8 x 5 mm) within 1 h of removing samples from the freezer. Tin capsules were dried at 60°C for 24 h, pinched closed, and analyzed by an isotope mass spectrometer PrecisION coupled with an elemental analyser C, N, and S VarioMicro (Elementar, Germany) at the Laboratory of Trophic and Isotopic Ecology, University of Liège.

2.3. Fatty acid extraction, quantification and CSIA

Fatty acid methyl esters (FAME) were prepared from freeze-dried samples using a direct transesterification procedure with 2.5% (v:v) sulfuric acid in methanol as described by De Troch et al. (2012). An internal standard (FA 19:0, 5 µg) was added prior to the transesterification procedure. FAME were extracted twice with hexane. The hexane was evaporated and the residue was dissolved in 200 µL hexane. Composition analysis of FA was carried out using a gas chromatograph (HP 7890B, Agilent Technologies, Diegem, Belgium) equipped with a flame ionization detector (FID) and connected to an Agilent 5977A Mass Selective Detector (Agilent Technologies, Diegem, Belgium). The GC was further equipped with a PTV injector (CIS-4, Gerstel, Mülheim an der Ruhr, Germany). A 60 m × 0.25 mm × 0.20 µm film thickness HP88 fused-silica capillary column (Agilent Technologies, Diegem, Belgium) was used for the gas chromatographic analysis, at a constant Helium flow rate (2 mL min⁻¹). The injected sample is split equally between the MS and FID detectors at the end of the GC column using an Agilent capillary flow technology splitter. The oven temperature program was as follows: at the time of sample injection the column temperature was 50°C for 2 min, then gradually increased at 30°C min⁻¹ to 180°C, followed by a second increase at 2°C min⁻¹ to 230°C. The injection volume was 2 µL. The injector temperature was held at 30°C for 0.1 min and then ramped at 10°C s⁻¹ to 250°C and held for 10 min. The transfer line for the column was maintained at 250°C. The quadrupole and ion source temperatures were 150 and 230°C, respectively. Mass spectra were recorded at 70 eV ionization voltage over the mass range of 50–550 m/z units. FAME were analyzed with the GC-MS prior to CSIA due to the higher total FA profile resolution and detection capabilities. Chromatogram analysis was done with Agilent MassHunter Quantitative Analysis software (Agilent Technologies, Diegem, Belgium). The signal obtained with the FID detector was used to generate quantitative data of all compounds. Peaks were identified based on the combination of their retention times, compared with external standards as a reference (Supelco 37 Component FAME Mix, Sigma-Aldrich, Overijse, Belgium) and the mass spectra obtained with the Mass Selective Detector. Quantification of FAME was based on the FID area of the internal standard (19:0) and on the conversion of peak areas to the amount of the FA by a theoretical response factor for each FA (Ackman and Sipos 1964; Wolff et al. 1995).

To assess the ^{13}C within the FAs, FAMEs from all treatments and field samples were analyzed by capillary gas chromatography combustion-isotope ratio mass spectrometry (GC-c-IRMS) at the Isotope Bioscience Laboratory (ISOFYS), Ghent University. The GC-c-IRMS system consisted of a Trace GC 1310 equipped with a PTV injector and a VF23-MS column (length = 60 m, ID = 0.25 mm, film = 0.25 µm), connected to

combustion/pyrolysis unit (GC-ISOLINK) where the FAME are converted to CO₂. The FAME is let by an automated open split system (Conflo IV) to an IRMS detector (DeltaV advantage, Thermo Scientific, Bremen Germany). During injection, the PTV was set at 50°C and heated to 280°C at a rate of 10°C s⁻¹, with a cleaning phase at 350°C and flow set at 1.2 mL. The GC column was kept at 50°C for 2 min, heated to 150°C at a rate of 50°C min⁻¹, then heated to 210°C at 1.5°C min⁻¹, during a final clearing phase the column was heated to 250°C and kept at that temp for 5 min. ¹³C abundance was calibrated using the F8-3 mix of Arndt Schimmelman. Typical precision of ¹³C abundance is within 0.0005%. The GC-c-IRMS was not able to determine the position of the unsaturation in the carbon-20 chain (20:1), therefore its full notation is not indicated in the figures and tables reported in the results section.

2.4. CSIA calculations

During GC-c-IRMS analysis the analytes are converted to CO₂ to be analysed by the IRMS detector where m/z 44, 45 and 46 are recorded simultaneously by three detectors. From the ratio of these three traces the *a*¹³C can be determined with high precision. The peak area (PA) of the individual FA can be used to also assess the FA content ([FA]). Commonly, in not artificially ¹³C enriched material this is done by using the combined peak area of the three mass traces. However, due to the high ¹³C enrichments and the different amplifications of the detectors, the [FA] per copepod was determined as follows:

$$(1) [FA] = \left(\frac{PA_{44, FAME} \times (1 - a^{13}C_{IS})}{PA_{44, IS}} + \frac{PA_{45, FAME} \times (a^{13}C_{IS})}{PA_{45, IS}} \right) \times \frac{m_{IS} \times (nC_{IS}) \times M_{FA}}{M_{IS} \times (nC_{FA} + 1) \times N}$$

With $PA_{x, FAME}$ and $PA_{x, IS}$ being the peak area at m/z = x of the FAME of interest and of the internal standard (IS), respectively, $a^{13}C_{IS}$ the ¹³C abundance in the IS (1.08%), m_{IS} the mass of the C19:0-FAME added (50 µg), M_{FA} and M_{IS} the molar mass of the FA of interest and of the IS (312.54 g•mol⁻¹), respectively, nC_{FA} and nC_{IS} indicating the number of carbons in the FA of interest and in IS (20), and N being the number of copepods in the extracted sample.

The GC-c-IRMS measurements delivers the ¹³C abundance of the individual FAME ($a^{13}C_{FAME}$). To obtain the *a*¹³C of the corresponding FA ($a^{13}C_{FA}$), the measured $a^{13}C_{FAME}$ must be corrected for the contribution of the methyl ($a^{13}C_{MeOH}$), added during derivatization to FAME:

$$(2) a^{13}C_{FA} = \frac{[a^{13}C_{FAME} \times (nC_{FA} + 1) - a^{13}C_{MeOH}]}{nC_{FA}}$$

The fraction of carbon assimilated ($f_{C\text{ assi}}$) in consumer FAs derived from the ¹³C-labelled *D. tertiolecta* can be computed as:

$$f_{Cassi} = \frac{a^{13}C_{FA-exp.} - a^{13}C_{FA-control}}{a^{13}C_{labelledDUNA} - a^{13}C_{fieldfood}}$$

(3)

With $a^{13}C_{FA-exp.}$ and $a^{13}C_{FA-control}$ representing the $a^{13}C_{FA}$ of the specific FA in copepods fed with ^{13}C -labelled *D. tertiolecta* and control copepod (directly collected on field site), respectively, $a^{13}C_{labelled DUNA}$ and $a^{13}C_{field food}$ (1.08‰) indicating the bulk $a^{13}C$ of the ^{13}C -labelled *D. tertiolecta* and of the food prior to incubation, respectively (adapted from Werbrouck et al. 2017). The bulk ^{13}C of the labelled *D. tertiolecta*, was not measured due to instrumental limitations to measure very high enrichments, therefore the $a^{13}C_{labelled DUNA}$ was estimated using the $a^{13}C_{FA}$ of 18:3 ω 3 (46.45%) found in the calanoid copepod samples. This value was used as a proxy due to the high concentration of 18:3 ω 3 in *D. tertiolecta* (Thor et al. 2007), and high uptake by *T. longicornis*. Finally, the absolute amount of FA derived from the carbon assimilated of the ^{13}C -labelled *D. tertiolecta* ($[FA]_{Cassi}$) could be computed as follows:

$$[FA]_{Cassi} = [FA] \times f_{Cassi}$$

(4)

For FAs already present in *D. tertiolecta* (SFA, MUFAs and PUFAs > 20 carbon units), we assume that labelled FAs in the copepods are a combination of direct unaltered incorporation, biosynthesis and conversion. LC-PUFAs (ARA, EPA and DHA) are not present in *D. tertiolecta*, therefore labelled LC-PUFAs in the copepod are the result of biosynthesis from dietary obtained FAs (see Supplementary Information, Table S1). The carbon assimilation from the algae into the total sum of all measured FAs (TFA) relative to the absolute concentrations was additionally calculated.

2.5. Statistical analysis

All statistical analyses and visualizations were conducted in R, version 4.1.1 (R Core Team 2021). Intra-specific cell concentrations of *D. tertiolecta* between day 1 and 6 were compared using a Bonferroni corrected multiple pairwise t-test. No increase of algae concentrations during the experimental treatment was detected, therefore algae growth inhibition was considered successful (Fig. S1). Relative percent FA composition data were analyzed using non-parametric multidimensional scaling (nMDS), Bray-Curtis dissimilarity, on cube-root transformed data. A permutational analysis of variance (PERMANOVA) was conducted based on groups determined by hierarchical clustering. To discriminate which FAs were contributing the most to these differences, a similarity percentages test (SIMPER) was conducted.

A quasi-binomial logistic generalized linear model (GLM) was used to model proportional copepod survival along temperature, considering species identity as a factor and weighted by the number of copepods in each sample, to account for an overdispersion of the data estimated by the ratio of the residuals deviance and the degrees of freedom (Haman 2020). Multiple comparisons of type Tukey were applied to the survival GLM, using the package 'multcomp' to determine significant differences considering species and temperature (Hothorn et al. 2008). Due to the non-linear relationship, generalized

additive models (GAM) were applied to the relative carbon assimilation into the TFA ($C_{\text{asssi}} \text{TFA}^{-1}$) and the fraction of carbon assimilation into specific FAs using the package 'mgcv' (Wood 2011). Non-parametric smoothers (s) by restricted maximum likelihood were applied to the temperature effects (T) by species identity (S), considering species as a factor: $C_{\text{asssi}} \text{TFA}^{-1} \sim f(S) + s(T, \text{by} = S)$. These data violated homogeneity assumptions evaluated by the dispersion of the residuals versus fitted values, due to zero-inflation, therefore a gamma distribution family was assumed with a log-link function (Zuur et al. 2009), providing a better model to include differences between species (Table S3). The exception to this was 18:3 ω 3, which was entered into the gaussian GAM untransformed (link = identity). Due to high mortality the FA data from two *T. longicornis* replicates at 23°C have been omitted. Model selection was done on the basis of the Akaike Information Criterion (AIC) and ANOVA. The significance of the smooth terms are reported, and explained deviance is listed on the GAMs as it is considered as a generalized measurement of goodness of fit, rather than R^2 -values (Wood 2011). Some models could not be reliably interpreted for FAs with numerous undetected values and were omitted; therefore, caution should be exercised in the cases where sample quantities were below detection limits.

3. Results

3.1. Survival and diet characterization

The proportional survival can be predicted from the interaction between temperature (T) exposure and species (S) identity (GLM, $P = 0.003$) (Fig. 1). Accordingly, the effect of temperature on survival is species-specific. The harpacticoid, *P. littoralis*, survival was not significantly different ($94.8 \pm 4.1\%$) across all temperature treatments (GLM Tukey, 11:23°C, $P = 0.999$) (Table S3). In contrast, the survival of the calanoid, *T. longicornis*, had a clear negative relationship with temperature, ranging from $83.8 \pm 8.3\%$ at 11°C to $22.5 \pm 14.7\%$ at 23°C (GLM Tukey, $P < 0.01$) (Table S3).

3.2. Interspecific comparison of FA composition

Adult *T. longicornis* individuals are larger in size than *P. littoralis*, therefore relative FA content (fraction of TFA) will be used hereafter, instead of absolute content ($\text{ng individual}^{-1}$) (Table S4), to standardize prior to comparison between species. In *T. longicornis* FAs 16:0, 20:5 ω 3, and 22:6 ω 3 are the most abundant, comprising of $> 70\%$ of the total FA composition (Table S5). Comparatively, in *P. littoralis* FA 16:0, 16:1 ω 5, 16:1 ω 7, 20:5 ω 3, and 22:6 ω 3 are the most abundant, corresponding to $> 70\%$ of the total FA composition (Table S5). Differences in FA composition were apparent between all temperature treatments and field samples among species (PERMANOVA, $P = 0.012$). However, hierarchical clustering and nMDS visualization of the data showed these did not fall into natural groups, therefore only significant differences (PERMANOVA, $P = 0.001$) between broad field and experimental species groups were considered (Fig. S2). The FAs that contribute the most to the differences between species in the field are 20:5 ω 3, 14:0, 16:1 ω 5, 22:6 ω 3, and 16:1 ω 7 (Table S6). FAs 20:5 ω 3, 14:0 and 22:6 ω 3, are present in higher relative amounts in *T. longicornis* (Table S5). Accordingly, these same FAs also contribute largely

to the differences between the species experimental groups, as well as 18:3 ω 3, which is present in high amounts in the algal feed (*D. tertiolecta*, Table S1), 24:1 ω 9 and 18:1 ω 7 (Table S6).

Interestingly, there was no significant difference between the relative amounts of EPA in *P. littoralis* in the field and experimental samples, regardless of temperature treatment (Kruskal-Wallis, $P = 0.96$), whereas they decrease in *T. longicornis* (Kruskal-Wallis, $P = 0.031$) (Fig. 2a). Similarly, there is no difference between the relative amount of DHA in *P. littoralis*' field and experimental incubation samples, with the exception of treatments at 17 (Pairwise t-test, $P = 0.042$) and 23°C (Pairwise t-test, $P = 0.018$) (Fig. 2b). In *T. longicornis*, relative DHA values increased between field and experimental samples for temperatures 11 (Pairwise t-test, $P = 0.042$), 14 (Pairwise t-test, $P = 0.004$), 17 (Pairwise t-test, $P = 0.012$), and 20°C (Pairwise t-test, $P = 0.013$) with the exception of the treatment at 23°C (Pairwise t-test, $P = 0.22$).

3.3. Carbon assimilated into total fatty acids

As there was insufficient material for separate carbon isotope analysis for all treatments (Fig. S3), due to the high mortality of *T. longicornis*, carbon assimilation into the total fatty acids (TFA) will be considered as a proxy for bulk carbon uptake. The total carbon assimilated by *P. littoralis* during the experimental incubation, indicated by carbon assimilation derived from ^{13}C -labelled *D. tertiolecta*, into the total FA ($C_{\text{ass}} \text{TFA}^{-1}$) varied with increasing temperature (Fig. 3a). Carbon assimilated into the total consumer FAs decreased from $0.449 \pm 0.210\%$ at 11°C to $0.279 \pm 0.068\%$ at 20°C, then increased to $1.287 \pm 0.318\%$ at 23°C (GAM, $P < 0.001$). Comparatively, *T. longicornis* displayed a significantly higher relative carbon assimilation with a mean value of $12.084 \pm 4.617\%$, not significantly varying with increased temperatures (GAM, $P = 0.34$) (Fig. 3b).

3.4. Carbon assimilation per FA

Overall, *T. longicornis* displayed higher carbon assimilation, derived from *D. tertiolecta*, into its FA pool than *P. littoralis* per individual. Among the SFA, carbon assimilation into FAs 16:0 and 18:0 were most abundant. Carbon assimilation in 16:0 ranged from 0.269 ± 0.146 to $2.103 \pm 0.313 \text{ ng ind}^{-1}$ for *P. littoralis* and 28.74 ± 4.414 to $13.47 \pm 12.26 \text{ ng ind}^{-1}$ for *T. longicornis* at 11 to 23°C, respectively (Table S7). Carbon assimilation in 18:0 ranged from 0.014 ± 0.009 to $0.105 \pm 0.047 \text{ ng ind}^{-1}$ for *P. littoralis* and 1.664 ± 0.385 to $1.249 \pm 0.971 \text{ ng ind}^{-1}$ for *T. longicornis* at 11 to 23°C, respectively. 18:3 ω 3 was present in markedly high amounts in the *D. tertiolecta* feed (Table S1), and accordingly had higher incorporation values, reflective of consumption patterns. These values of 18:3 ω 3 ranged from 0.211 ± 0.176 to $1.891 \pm 0.371 \text{ ng ind}^{-1}$ in *P. littoralis* and 15.57 ± 5.475 to $3.168 \pm 6.337 \text{ ng ind}^{-1}$ in *T. longicornis* at 11 to 23°C, respectively.

Contribution of *D. tertiolecta* derived FA is temperature dependent in *P. littoralis* for all SFA assessed (14:0, 16:0 and 18:0) (GAM, $P < 0.001$) (Table S2), displaying a logistic relationship; increasing until 14°C and again past 20°C (Fig. 4a-c). Comparatively, *T. longicornis* only displays a temperature dependent relationship for SFA 14:0 (GAM, $P = 0.039$), peaking at 17°C. A similar pattern is observed in *T. longicornis*

for MUFA 16:1 ω 9 (GAM, $P < 0.001$), whereas there is no dependence on temperature for *P. littoralis* (GAM, $P = 0.978$). For MUFA and PUFA 18:1 ω 11 and 18:3 ω 3, respectively, there is a temperature dependent relationship for both species (18:1 ω 11 and 18:3 ω 3 GAM, *P. littoralis*: $P < 0.001$, *T. longicornis*: $P = 0.022$, $P = 0.018$) (Fig. 4d-f). Interestingly, we can observe contrasting responses of incorporation of 18:1 ω 11, as in *T. longicornis* its relative concentrations decrease with increased temperature while *P. littoralis* exhibits the opposite response, reaching similar levels as *T. longicornis* at 23°C. PUFA 18:3 ω 3 is dominant in the *D. tertiolecta* feed, thereby informing uptake and incorporation of the labelled feed. There is a significant increase in carbon incorporation for *P. littoralis* 18:3 ω 3 (1.891 ± 0.371 ng ind⁻¹) at 23°C with respect to lower temperature treatments: 11, 14, 17, 20°C (0.211 ± 0.176 , 0.524 ± 0.283 , 0.255 ± 0.116 , 0.174 ± 0.122 ng ind⁻¹, respectively), thereby reaching a more comparable carbon assimilation to *T. longicornis* at 23°C (3.168 ± 6.337 ng ind⁻¹).

3.4. Comparison of de novo production between species

T. longicornis displayed higher *de novo* production of both EPA and DHA than *P. littoralis* with an exception at 23°C (Table S7). *T. longicornis* EPA production ranged from 0.226 ± 0.117 to 0.030 ± 0.060 ng ind⁻¹ at 11 to 23°C, respectively. In comparison, EPA production in *P. littoralis* ranged from 0.015 ± 0.011 to 0.033 ± 0.008 ng ind⁻¹ at 11 to 23°C, respectively. Lower DHA than EPA production was observed ranging from 0.161 ± 0.043 to 0.012 ± 0.025 and from 0.009 ± 0.001 to 0.030 ± 0.019 ng ind⁻¹ in the temperature range from 11 to 23°C in *T. longicornis* and *P. littoralis*, respectively.

Since total amounts produced per individual are minimal in *P. littoralis* likely due to size differences with the calanoid and species-specific retention of field FA, we chose to model the relative percent *de novo* FAs (as a percentage of total FAs) to account for these discrepancies and to allow comparison. In terms of relative FA composition, there is a significant effect of temperature on the production of *de novo* EPA in *T. longicornis* (Fig. 5a). Comparatively, *P. littoralis* does not change EPA production with temperature with a mean value of 0.023 ng ind⁻¹ (no significant differences between treatments). Despite showing significant relationships for both species for the *de novo* produced DHA with temperature, due to the numerous undetected values resulting from low concentrations, the GAM constructed for this FA should be interpreted with caution (Fig. 5b). This is reflected in a low proportion of the variance and deviance explained ($R^2 = 0.219$, 68.0%).

4. Discussion

To compensate for poor quality food, organisms can increase ingestion rates (Malzahn and Boersma 2012), and their carbon incorporation efficiency (Gulati and Demott 1997). Through the use of labelled food we are able to discern this effect on the assimilation and thereby what is retained by the individuals. *T. longicornis* displayed higher overall assimilation, and maintains this across all test temperatures, likely to compensate for the high metabolic costs associated with the LC-PUFA deficient diet and warming pressure. Since the calanoid carbon assimilation did not significantly vary across the temperature range,

this indicates that either this process is not regulated (*i.e.*, independent of temperature), or the experimental stress was heightened enough at 11°C to induce maximum ingestion rates, assumed from carbon assimilation, to compensate for the temperature and diet stressors. In comparison, *P. littoralis* has relatively low assimilation rates, only increasing at the highest temperature treatment (23°C). This - in conjunction with the retention of the relative field LC-PUFA concentrations - may indicate that *P. littoralis* does not require to increase assimilation to meet their metabolic demands until the extreme of 23°C. The carbon assimilation rate in *P. littoralis* ranges from 0.075 to 0.214% day⁻¹ at 11 and 23°C, respectively, whereas it is on average 2.014% day⁻¹ for *T. longicornis*. Higher observed lipid assimilation rates have been recorded in Antarctic calanoid species *Calanoides acutus* and *Calanus propinquus* of 3.1 and 3.9% day⁻¹, respectively, when fed a diatom diet under natural temperature conditions (Graeve et al. 2020). The small herbivorous arctic calanoid *Pseudocalanus minutus* has demonstrated a more similar carbon assimilation rate to *T. longicornis* of 2.6% day⁻¹, while the cyclopoid *Oithona similis* has a carbon assimilation rate more similar to *P. littoralis* at 0.5% day⁻¹, when fed a diatom dinoflagellate mixture at 4°C (Boissonnot et al. 2016). These studies reporting the assimilation efficiency have been conducted under ambient sampling temperature and with higher food quality (presence of LC-PUFAs), therefore individuals may have increased their uptake in response to these favourable conditions. We suggest that the combined stress of a LC-PUFA deficient diet and higher temperatures resulted in reduced rates of carbon incorporation for two species of copepods of different orders, displaying a different functional trait and occurring in a different habitat. Additionally, the low assimilation rates in *P. littoralis* may be explained through the preferential use or ability to retain its own relative lipid content rather than utilization of the poor external food source. Interestingly, the deviation of *T. longicornis* carbon assimilation per TFA increased with temperature, whereas for *P. littoralis* replicates were quite similar. This increased variability is recognized as a biochemical indicator of environmental stress (Werbruck et al. 2017).

MUFA 20:1 ω 9 and 22:1 ω 11 are known to be produced by herbivorous copepods, which then get converted to fatty alcohols (Graeve et al. 1994). Increased production of these MUFA corresponds to higher ingestion and therefore assimilation of source FAs (Helenius et al. 2020b). For 20:1 we can observe minimal to undetected amounts for *P. littoralis*, however at 23°C this significantly increased, implying that individuals have increased production to cope with the higher metabolic demands. In contrast, higher amounts are recorded in *T. longicornis* decreasing with increasing temperature from 14 to 17°C. After this point 20:1 becomes undetectable in the 20 and 23°C temperature treatments. This suggests that beyond 17°C these primary conversion processes and increased ingestion are no longer possible to offset the metabolic demand, and mortality is induced. This is in accordance with the carbon assimilation results.

In our study, 18:3 ω 3 (ALA) is considered as a proxy for *D. tertiolecta* uptake, being the dominant FA in the feed and highly reduced in the field samples. Therefore, the primary origin of this FA is proposed to be through direct incorporation from experimental feeding, and minimal amounts through modification. Using *D. tertiolecta* however also implies that we are not able to quantify copepod bioconversion of

MUFAs into short-chain PUFAs (*i.e.*, linoleic acid (LA, 18:2 ω 6), ALA) by methyl-end desaturases. Notably, the carbon assimilation into ALA does not vary with temperature for *T. longicornis*, with levels remaining around 100% (\pm 9.65), indicating all ALA in *T. longicornis* is derived from its diet. Increased variability between samples can be caused by undigested algae in the gut, the high $a^{13}C$ values resulting in increased instrument uncertainty on the quantification, or can also indicate modification from other FAs. Therefore, in future experiments it is suggested to increase the experimental incubation and allow more time for gut clearance, potentially 24 h starved after exposure, to ensure the $a^{13}C$ reading is solely representative of assimilated carbon. Alternatively, baker's yeast could be used instead of *D. tertiolecta*, as it contains no or very few 18:3 ω 3 and no other LC-PUFAs (Payne and Rippingale 2000; Nielsen et al. 2020). Interestingly, in *P. littoralis* the carbon assimilation into 18:3 ω 3 does have a significant positive relationship with temperature, increasing incorporation reaching similar levels as *T. longicornis* only at 23°C (93.47 \pm 10.18%). This suggests that *P. littoralis* increased ingestion of the labelled *D. tertiolecta* as temperatures increased, whereas *T. longicornis* maintained the same uptake throughout, similarly to the TFA carbon assimilation values. Since the calanoid displays high ingestion and/or incorporation of the labelled feed at all temperatures, we can deduce that the stress of a poor quality diet and temperature was already being compensated for at 11°C (Calliari and Tiselius 2005). We can observe that although *T. longicornis* exhibits higher carbon incorporation into its FAs, this compensation is not enough to make up for the overall loss of absolute FA concentration, which is apparent looking at its absolute EPA and DHA content. The biosynthesis recorded under these experimental temperatures indicate that both species were not producing sufficient *de novo* EPA and DHA under LC-PUFA deficient conditions to restore their ω 3-stocks, similarly recorded by Werbrouck et al. (2017).

To compare between species we must consider their thermal limits, and the typical stressors organisms face in their natural environment. Our results indicate that the harpacticoid, *P. littoralis*, appears to be more suited to more variable conditions than the calanoid *T. longicornis*. The differing lifestyles of pelagic calanoids and benthic harpacticoids can be linked to the prey types encountered, the frequency of feeding periods, and the energy demands throughout their lifespan. Calanoids have more seasonal variability affecting feeding periods, therefore overwintering strategies, *i.e.*, diapause, are often necessary (Pond et al. 2012). Subsequently, there are tendencies to store wax esters prior to these periods. As the *T. longicornis* individuals were sampled mid-February, and likely pre-spring bloom conditions, *T. longicornis* contained higher amounts of both DHA and EPA than *P. littoralis*, indicative of a mixed diet of dinoflagellates and diatoms. Comparatively, harpacticoids have access to and can thus utilize more variable food sources, optimizing on detrital and bacterial nutrients that are available year-round. Consequently, *P. littoralis* from the field contained higher relative amounts of 16:1 ω 7 and 16:1 ω 5, suggesting herbivorous feeding on microphytobenthos (Graeve et al. 1994), and 18:1 ω 7, implying bacterial feeding (Conway and McDowell Capuzzo 1991). Therefore, the energy stores in which these individuals entered the experiment are quite contrasting due to the differences in the available prey field and life histories. Since *P. littoralis* occupies the benthos, this species is more sedentary and expends less energy in comparison to *T. longicornis*' vertical movement throughout the water column (Hays et al. 2001). However, calanoids in the pelagic environment also experience temperature buffering effects when

occupying the water column. Therefore, when a temperature change occurs it happens at a slower rate, potentially allowing for either individual displacement (possible by their higher vertical mobility) or restructuring of their FA composition. As such, the intertidal conditions that the harpacticoids inhabit are much harsher. The temperature change can be more stochastic, and ranges between 4 and 22°C throughout the year (Sahan et al. 2007). This justifies their eurythermic response, *i.e.*, ability to tolerate a wide temperature range, compared to *T. longicornis*' more stenothermic survival response. The overall outcome of this study suggests that based on their FA dynamics the benthic harpacticoid, *P. littoralis*, has a greater potential for resilience under more extreme conditions.

5. Conclusions

P. littoralis did not assimilate dietary carbon readily, and thus had a LC-PUFA bioconversion rate that is lower than what is found in other copepods (Boissonnot et al. 2016; Graeve et al. 2020). *T. longicornis* displayed higher rates of *de novo* bioconversion for eicosapentaenoic acid (EPA, 20:5 ω 3) and docosahexaenoic acid (DHA, 22:6 ω 3) than *P. littoralis* at all temperatures, with the exception of DHA at 23°C. This temperature was the most stressful for the calanoid displaying a higher mortality with warming. Comparatively, the harpacticoid was eurythermal, with survival independent of temperature. The relative amount of EPA in *P. littoralis* did not change between the field and the experimental treatments. Therefore we hypothesize that this species is able to maintain the required amounts of EPA, thus not needing to allocate more energy than necessary towards these costly metabolic processes.

Although there may be a reduction in absolute ω 3 LC-PUFA availability in primary producers, it is important to consider that complete absence, as in our experiment, is not a realistic scenario. Despite the fact that *T. longicornis* demonstrated higher *de novo* production, albeit not in sufficient amounts, individuals depleted their field EPA stores more rapidly. This indicates that *T. longicornis* is not able to biosynthesize EPA at a rate necessary for basic metabolic functioning. Conversely, *P. littoralis* has maintained its relative storage, suggesting these extremes are within their coping capacity. Under the stressors imposed, *P. littoralis* has a greater potential for resilience when faced with extreme temperature conditions in comparison to *T. longicornis*. If significant, these bioconversion abilities in primary consumers have the capacity to upgrade a poor quality food source. As such, under LC-PUFA reduced conditions due to a changing climate, these capabilities could provide a source of EFA for higher trophic levels and should be considered in other species. This is the first experiment to quantify the *de novo* production of LC-PUFA in the dominant North Sea calanoid *T. longicornis* and monitor EFA *de novo* production along a thermal gradient in a comparative study with both harpacticoid and calanoid copepods.

Declarations

Compliance with ethical standards

The authors declare no conflict of interest and consent to the publication of this manuscript. No specialized permission was required for field sampling in both public and unprotected locations. Endangered or protected species were not involved in this project.

Acknowledgements

We thank Dr. Bruno Vlaeminck, Marine Biology Research Group, UGent for assisting with the fatty acid extraction/analysis, and Dr. Gilles Lepoint, Lab of Trophic and Isotope Ecology, ULiège for help with the bulk carbon stable isotope analysis. This research was supported with infrastructure funded by EMBC Belgium - FWO international research infrastructure I001621N. The first author is backed by a Bijzonder Onderzoeksfonds, Special Research Fund PhD grant – BOF, from Ghent University (BOF21/DOC/228), and the second author by a fundamental research PhD grant from the Research Foundation Flanders – FWO (11E2320N).

References

1. Ackman RG, Sipos JC (1964) Application of specific response factors in the gas chromatographic analysis of methyl esters of fatty acids with flame ionization detectors. *J Am Oil Chemists' Soc* 41:377–378. doi: 10.1007/BF02654818
2. Arendt KE, Jónasdóttir SH, Hansen PJ, Gärtner S (2005) Effects of dietary fatty acids on the reproductive success of the calanoid copepod *Temora longicornis*. *Mar Biol*. doi: 10.1007/s00227-004-1457-9
3. Beaugrand G, Reid PC, Ibañez F, Lindley JA, Edwards M (2002) Reorganization of North Atlantic Marine Copepod Biodiversity and Climate. *Science* 296:1692–1694. doi: 10.1126/science.1071329
4. Beaugrand G, Brander KM, Alistair Lindley J, Souissi S, Reid PC (2003) Plankton effect on cod recruitment in the North Sea. *Nature* 426:661–664. doi: 10.1038/nature02164
5. Bell MV, Tocher DR (2009) Biosynthesis of polyunsaturated fatty acids in aquatic ecosystems: general pathways and new directions. In: Kainz M, Brett MT, Arts MT (eds) *Lipids in Aquatic Ecosystems*. Springer New York, New York, NY, pp 211–236
6. Bell MV, Dick JR, Anderson TR, Pond DW (2007) Application of liposome and stable isotope tracer techniques to study polyunsaturated fatty acid biosynthesis in marine zooplankton. *J Plankton Res* 29:417–422. doi: 10.1093/plankt/fbm025
7. Bertram DF, Mackas DL, Welch DW, Boyd WS, Ryder JL, Galbraith M, Hedd A, Morgan K, O'Hara PD (2017) Variation in zooplankton prey distribution determines marine foraging distributions of breeding Cassin's Auklet. *Deep Sea Res Part I* 129:32–40. doi: 10.1016/j.dsr.2017.09.004
8. Boissonnot L, Niehoff B, Hagen W, Søreide JE, Graeve M (2016) Lipid turnover reflects life-cycle strategies of small-sized Arctic copepods. *J Plankton Res*. doi: 10.1093/plankt/fbw076
9. Calliari D, Tiselius P (2005) Feeding and reproduction in a small calanoid copepod: *Acartia clausi* can compensate quality with quantity. *Mar Ecol Prog Ser* 298:241–250. doi: 10.3354/meps298241

10. Cnudde C, Moens T, Werbrouck E, Lepoint G, Van Gansbeke D, De Troch M (2015) Trophodynamics of estuarine intertidal harpacticoid copepods based on stable isotope composition and fatty acid profiles. *Mar Ecol Prog Ser* 524:225–239. doi: 10.3354/meps11161
11. Colombo SM, Rodgers TFM, Diamond ML, Bazinet RP, Arts MT (2020) Projected declines in global DHA availability for human consumption as a result of global warming. *Ambio* 49:865–880. doi: 10.1007/s13280-019-01234-6
12. Conway N, McDowell Capuzzo J (1991) Incorporation and utilization of bacterial lipids in the *Solemya velum* symbiosis. *Mar Biol* 108:277–291. doi: 10.1007/BF01344343
13. Coull BC (1990) Are Members of the Meiofauna Food for Higher Trophic Levels? *Transactions of the American Microscopical Society*. doi: 10.2307/3226794
14. Cronin TW, Fasick JI, Schweikert LE, Johnsen S, Kezmoh LJ, Baumgartner MF (2017) Coping with copepods: do right whales (*Eubalaena glacialis*) forage visually in dark waters? *Philosophical Transactions of the Royal Society B: Biological Sciences* 372:20160067–20160067. doi: 10.1098/rstb.2016.0067
15. Daase M, Falk-Petersen S, Varpe Ø, Darnis G, Søreide JE, Wold A, Leu E, Berge J, Philippe B, Fortier L (2013) Timing of reproductive events in the marine copepod *Calanus glacialis*: A pan-Arctic perspective. *Canadian Journal of Fisheries and Aquatic Sciences* 70:871–884. doi: 10.1139/cjfas-2012-0401
16. De Troch M, Boeckx P, Cnudde C, Van Gansbeke D, Vanreusel A, Vincx M, Caramujo MJ (2012) Bioconversion of fatty acids at the basis of marine food webs: Insights from a compound-specific stable isotope analysis. *Marine Ecology Progress Series* 10.3354/meps09920
17. Deschutter Y, De Schamphelaere K, Everaert G, Mensens C, De Troch M (2019) Seasonal and spatial fatty acid profiling of the calanoid copepods *Temora longicornis* and *Acartia clausi* linked to environmental stressors in the North Sea. *Marine Environmental Research*. doi: 10.1016/j.marenvres.2018.12.008
18. Frederiksen M, Anker-Nilssen T, Beaugrand G, Wanless S (2013) Climate, copepods and seabirds in the boreal Northeast Atlantic - current state and future outlook. *Global Change Biology*. doi: 10.1111/gcb.12072
19. Garzke J, Ismar SMH, Sommer U (2015) Climate change affects low trophic level marine consumers: warming decreases copepod size and abundance. *Oecologia* 177:849–860. doi: 10.1007/s00442-014-3130-4
20. Garzke J, Hansen T, Ismar SMH, Sommer U (2016) Combined effects of ocean warming and acidification on copepod abundance, body size and fatty acid content. *PLoS ONE*. doi: 10.1371/journal.pone.0155952
21. Gee JM (1987) Impact of epibenthic predation on estuarine intertidal harpacticoid copepod populations. *Mar Biol*. doi: 10.1007/BF00397967
22. Graeve M, Kattner G, Hagen W (1994) Diet-induced changes in the fatty acid composition of Arctic herbivorous copepods: Experimental evidence of trophic markers. *Journal of Experimental Marine Biology and Ecology* 182:97–110. doi: 10.1016/0022-0981(94)90213-5
23. Graeve M, Boissonnot L, Niehoff B, Hagen W, Kattner G (2020) Assimilation and turnover rates of lipid compounds in dominant Antarctic copepods fed with ¹³C-enriched diatoms. *Philosophical*

24. Gulati R, Demott W (1997) The role of food quality for zooplankton: remarks on the state-of-the-art, perspectives and priorities. *Freshw Biol* 38:753–768
25. Haman J (2020) Quasibinomial model in R glm(). In: Random Effect. <https://randomeffect.net/post/2020/10/12/quasi-binomial-in-r-glm/>
26. Hays GC, Kennedy H, Frost BW (2001) Individual variability in diel vertical migration of a marine copepod: Why some individuals remain at depth when others migrate. *Limnol Oceanogr* 46:2050–2054. doi: 10.4319/lo.2001.46.8.2050
27. Helenius L, Budge SM, Nadeau H, Johnson CL (2020a) Ambient temperature and algal prey type affect essential fatty acid incorporation and trophic upgrading in a herbivorous marine copepod. *Philosophical Trans Royal Soc B: Biol Sci*. doi: 10.1098/rstb.2020.0039
28. Helenius L, Budge SM, Johnson CL (2020b) Stable isotope labeling reveals patterns in essential fatty acid growth efficiency in a lipid-poor coastal calanoid copepod. *Mar Biol* 167:178–178. doi: 10.1007/s00227-020-03794-8
29. Hixson SM, Arts MT (2016) Climate warming is predicted to reduce omega-3, long-chain, polyunsaturated fatty acid production in phytoplankton. *Global change biology*. doi: 10.1111/gcb.13295
30. Hothorn T, Bretz F, Westfall P (2008) Simultaneous Inference in General Parametric Models. *Biom J* 50:346–363
31. Jónasdóttir SH, Visser AW, Richardson K, Heath MR (2015) Seasonal copepod lipid pump promotes carbon sequestration in the deep North Atlantic. *Proceedings of the National Academy of Sciences* 112:12122–12126. doi: 10.1073/pnas.1512110112
32. Kabeya N, Fonseca MM, Ferrier DEK, Navarro JC, Bay LK, Francis DS, Tocher DR, Filipe L, Castro C, Monroig Ó (2018) Genes for de novo biosynthesis of omega-3 polyunsaturated fatty acids are widespread in animals
33. Kabeya N, Ogino M, Ushio H, Haga Y, Satoh S, Navarro JC, Monroig Ó (2021) A complete enzymatic capacity for biosynthesis of docosahexaenoic acid (DHA, 22: 6n-3) exists in the marine Harpacticoida copepod *Tigriopus californicus*. *Open Biology*. doi: 10.1098/rsob.200402
34. Kattner G, Hagen W (2009) Lipids in marine copepods: latitudinal characteristics and perspective to global warming. *Lipids in Aquatic Ecosystems*. Springer New York, New York, NY, pp 257–280
35. Koski M, Klein Breteler WCM (2003) Influence of diet on copepod survival in the laboratory. *Marine Ecology Progress Series* 10.3354/meps264073
36. Kwiatkowski L, Torres O, Bopp L, Aumont O, Chamberlain M, Christian JR, Dunne JP, Gehlen M, Ilyina T, John JG, Lenton A, Li H, Lovenduski NS, Orr JC, Palmieri J, Santana-Falcón Y, Schwinger J, Séférian R, Stock CA, Tagliabue A, Takano Y, Tjiputra J, Toyama K, Tsujino H, Watanabe M, Yamamoto A, Yool A, Ziehn T (2020) Twenty-first century ocean warming, acidification, deoxygenation, and upper-ocean nutrient and primary production decline from CMIP6 model projections. *Biogeosciences* 17:3439–3470. doi: 10.5194/bg-17-3439-2020

37. Lampitt RS, Noji T, Von Bodungen B (1990) What happens to zooplankton faecal pellets? Implications for material flux. Springer-Verlag
38. Lee MC, Choi BS, Kim MS, Yoon DS, Park JC, Kim S, Lee JS (2020) An improved genome assembly and annotation of the Antarctic copepod *Tigriopus kingsejongensis* and comparison of fatty acid metabolism between *T. kingsejongensis* and the temperate copepod *T. japonicus*. *Comparative Biochemistry and Physiology - Part D: Genomics and Proteomics*. 10.1016/j.cbd.2020.100703
39. Malzahn AM, Boersma M (2012) Effects of poor food quality on copepod growth are dose dependent and non-reversible. *Oikos* 121:1408–1416. doi: 10.1111/j.1600-0706.2011.20186.x
40. McGinty N, Barton AD, Record NR, Finkel ZV, Johns DG, Stock CA, Irwin AJ (2021) Anthropogenic climate change impacts on copepod trait biogeography. *Glob Change Biol* 27:1431–1442. doi: 10.1111/gcb.15499
41. Meyer JL (1994) The microbial loop in flowing waters. *Microbial Ecology*. doi: 10.1007/BF00166808
42. Monroig Ó, Kabeya N (2018) Desaturases and elongases involved in polyunsaturated fatty acid biosynthesis in aquatic invertebrates: a comprehensive review. *Fish Sci* 84:911–928. doi: 10.1007/s12562-018-1254-x
43. Moreno VJ, De Moreno JEA, Brenner RR (1979) Fatty acid metabolism in the calanoid copepod *Paracalanus parvus*: 1. Polyunsaturated fatty acids. *Lipids* 14:313–317. doi: 10.1007/BF02533413
44. Nielsen BLH, Gøtterup L, Jørgensen TS, Hansen BW, Hansen LH, Mortensen J, Jepsen PM (2019) n-3 PUFA biosynthesis by the copepod *Apocyclops royi* documented using fatty acid profile analysis and gene expression analysis. *Biology Open*. doi: 10.1242/bio.038331
45. Nielsen BLH, van Someren Gréve H, Rayner TA, Hansen BW (2020) Biochemical adaptation by the tropical copepods *apocyclops royi* and *pseudodiaptomus annandalei* to a pufa-poor brackish water habitat. *Mar Ecol Prog Ser* 655:77–89. doi: 10.3354/meps13536
46. Payne MF, Rippingale RJ (2000) Evaluation of diets for culture of the calanoid copepod *Gladioferens imparipes*. *Aquaculture* 187:85–96. doi: 10.1016/S0044-8486(99)00391-9
47. Pond DW, Tarling GA, Ward P, Mayor DJ (2012) Wax ester composition influences the diapause patterns in the copepod *Calanoides acutus*. *Deep-Sea Research Part II: Topical Studies in Oceanography*. 10.1016/j.dsr2.2011.05.009
48. R Core Team (2021) R: A language and environment for statistical computing. R Foundation for Statistical Computing, Vienna, Austria
49. Ratnayake WMN, Galli C (2009) Fat and Fatty Acid Terminology, Methods of Analysis and Fat Digestion and Metabolism: A Background Review Paper. *Ann Nutr Metab* 55:8–43. doi: 10.1159/000228994
50. Richardson AJ (2008) In hot water: Zooplankton and climate change
51. Sahan E, Sabbe K, Creach V, Hernandez-Raquet G, Vyverman W, Stal LJ, Muyzer G (2007) Community structure and seasonal dynamics of diatom biofilms and associated grazers in intertidal mudflats. *Aquat Microb Ecol*. doi: 10.3354/ame047253

52. Semmouri I, De Schampheleere KAC, Willemse S, Vandegheuchte MB, Janssen CR, Asselman J (2021) Metabarcoding reveals hidden species and improves identification of marine zooplankton communities in the North Sea. *ICES J Mar Sci* 78:3411–3427. doi: 10.1093/icesjms/fsaa256
53. Stenseth NC, Mysterud A, Ottersen G, Hurrell JW, Chan K-S, Lima M (2002) Ecological Effects of Climate Fluctuations. *Science* 297:1292–1296. doi: 10.1126/science.1071281
54. Stock W, Heylen K, Sabbe K, Willems A, De Troch M (2014) Interactions between benthic copepods, bacteria and diatoms promote nitrogen retention in intertidal marine sediments. *PLoS ONE*. doi: 10.1371/journal.pone.0111001
55. Thor P, Koski M, Tang K, Jónasdóttir S (2007) Supplemental effects of diet mixing on absorption of ingested organic carbon in the marine copepod *Acartia tonsa*. *Mar Ecol Prog Ser* 331:131–138. doi: 10.3354/meps331131
56. Turner JT (2004) The importance of small planktonic copepods and their roles in pelagic marine food webs
57. Twining CW, Taipale SJ, Ruess L, Bec A, Martin-Creuzburg D, Kainz MJ (2020) Stable isotopes of fatty acids: current and future perspectives for advancing trophic ecology. *Phil Trans R Soc B* 375:20190641. doi: 10.1098/rstb.2019.0641
58. Veloza AJ, Chu FLE, Tang KW (2006) Trophic modification of essential fatty acids by heterotrophic protists and its effects on the fatty acid composition of the copepod *Acartia tonsa*. *Mar Biol*. doi: 10.1007/s00227-005-0123-1
59. Werbrouck E, Bodé S, Van Gansbeke D, Vanreusel A, De Troch M (2017) Fatty acid recovery after starvation: insights into the fatty acid conversion capabilities of a benthic copepod (Copepoda, Harpacticoida). *Marine Biology*. 10.1007/s00227-017-3181-2
60. Wolff RL, Bayard CC, Fabien RJ (1995) Evaluation of sequential methods for the determination of butterfat fatty acid composition with emphasis on trans – 18:1 acids. Application to the study of seasonal variations in french butters. *J Am Oil Chemists' Soc* 72:1471–1483. doi: 10.1007/BF02577840
61. Wood SN (2011) Fast stable restricted maximum likelihood and marginal likelihood estimation of semiparametric generalized linear models. *J Royal Stat Society: Ser. B (Statistical Methodology)*doi: 10.1111/j.1467-9868.2010.00749.x

Figures

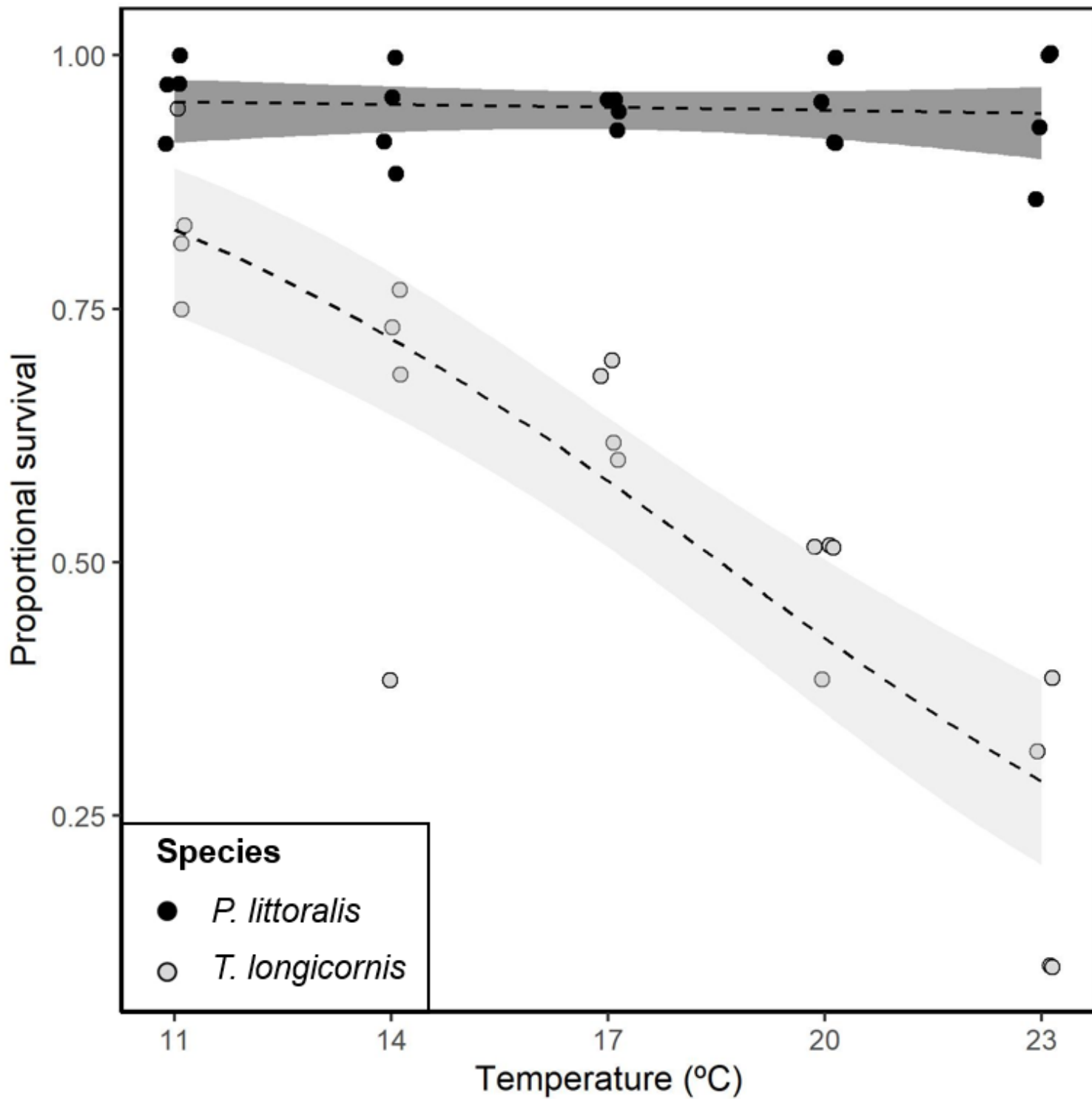


Figure 1

Generalized linear model of proportional survival for *P. littoralis* and *T. longicornis* along a temperature gradient

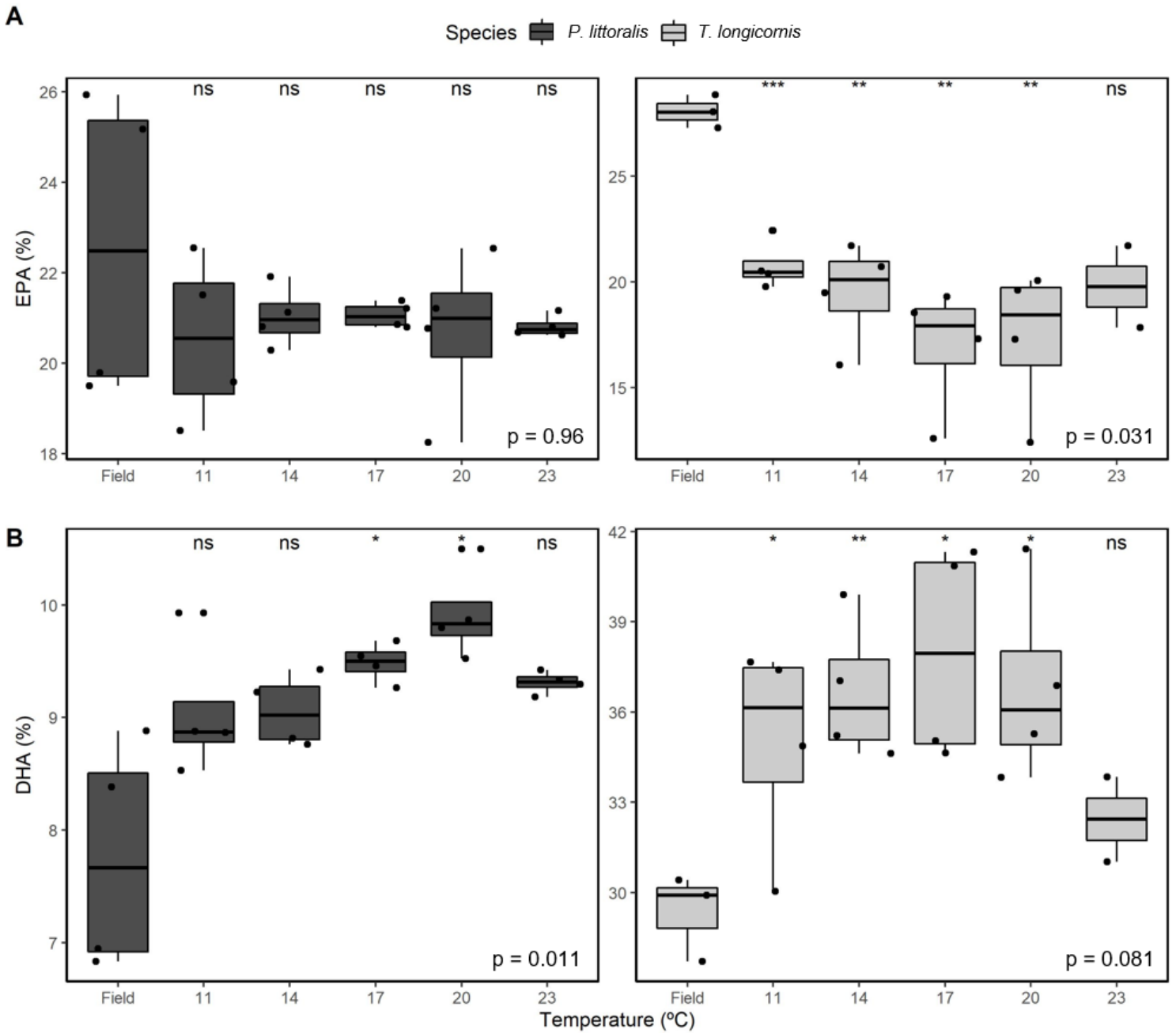


Figure 2

Relative (a) EPA and (b) DHA concentrations to the total FA in *P. littoralis* and *T. longicornis* from the field and across all temperature treatments (11, 14, 17, 20, and 23°C). Pairwise t-test performed for all temperature treatments against natural reference ('Field') group (n.s. = non-significant), and global Kruskal-Wallis p-value displayed on the bottom right

Figure 3

Fraction of the total fatty acids carbon derived from the labeled *D. tertiolecta* ($C_{\text{ass}} \text{TFA}^{-1}$) in (a) *P. littoralis* and (b) *T. longicornis* along a temperature gradient. Data displayed are untransformed and separated by species factor for clarity, with explained deviance displayed in right-corner representing log-transformed GAM model output described in text

Figure 4

GAMs displaying fraction of carbon assimilation per saturated FA (SFA): (a) 14:0, (b) 16:0, (c) 18:0, monounsaturated FA (MUFA): (d) 16:1 ω 9, (e) 18:1 ω 11, and polyunsaturated FA: (f) 18:3 ω 3 measured in *P. littoralis* '●' and *T. longicornis* '●' copepods along a temperature gradient. Apart from 18:3 ω 3, which is presented untransformed, carbon assimilation into FA are log-transformed; refer to Table S2 for significance, transformations, and model parameter information. Explained deviance is listed in the bottom right of each model

Figure 5

GAMs displaying fraction of carbon assimilation into de novo essential fatty acids (EFAs): (A) 20:5 ω 3 and (B) 22:6 ω 3 log-transformed in *P. littoralis* '●' and *T. longicornis* '●' copepods along a temperature gradient. Refer to Table S2 for significance, transformations, and model parameter information. Explained deviance is listed in the bottom right of each model

Supplementary Files

This is a list of supplementary files associated with this preprint. Click to download.

- [SISahota2022May5.docx](#)